Mar Biotechnol (2008) 10:701–708
DOI 10.1007/s10126-008-9108-7

ORIGINAL ARTICLE

Surface Display of GFP by *Pseudomonas Syringae* Truncated Ice Nucleation Protein in Attenuated *Vibrio Anguillarum* Strain

Yuzhou Xu · Qin Liu · Lingyun Zhou
Zhao Yang · Yuanxing Zhang

Received: 17 September 2007 / Accepted: 16 April 2008 / Published online: 6 June 2008

Abstract Microbial cell surface display of foreign proteins has been widely developed for many potential applications in live vaccine construction, whole-cell biocatalysts, and bioadsorption. To investigate the feasibility of displaying heterologous proteins on the surface of attenuated *Vibrio anguillarum* strain for potential multivalent live vaccine development, different display systems were built upon a truncated ice nucleation protein (INP) from *Pseudomonas syringae* ICMP3023 whose N- and C-terminal domains were considered to be the putative membrane-anchoring motifs. Green fluorescent protein (GFP), as a reporter, was fused with the display systems in different forms of N-GFP, NC-GFP, and N-GFP-C. Analysis of the total expression level and surface localization of GFP demonstrated that the truncated *P. syringae* INP could be used to display foreign protein in *V. anguillarum*, while the system of N-GFP showed the higher levels of total expression and surface display based on unit cell density among the three and might be available for further carrier vaccine development.

Keywords Bacterial cell surface display · Ice nucleation protein · Green fluorescent protein · *Vibrio anguillarum*

Introduction

Surface display of heterologous peptide and protein such as receptor, antigen, and enzyme in live bacterial cells is of considerable value for various biotechnological and industrial applications. Some examples are live vaccine development (Liljeqvist et al. 1997; Lee et al. 2000), whole-cell biocatalyst (Richins et al. 1997; Catherine et al. 2002), bioadsorbent (Xu and Lee 1999), and combinatorial library screening (Boder and Wittrup 1997).

Various outer membrane proteins serve as anchoring motifs for surface display, such as IgA1, AIDA-I, PAL, SpA, Lpp-OmpA, ice nucleation protein (INP), TraT, EaeA, OmpC, LamB, and FimH (Sang et al. 2003). INP is an outer membrane protein found in *Erwinia*, *Pseudomonas*, and *Xanthomonas*. The representative INP from *Pseudomonas syringae* is composed of three domains structurally distinguished as the nonrepetitive N- and C-terminal domains and a repetitive central domain (Graether and Jia 2001). The N-terminal domain (N, 175 residues) and C-terminal domain (C, 49 residues) are respectively believed to anchor the protein to the outer membrane (Graether and Jia 2001). Among the several identified INPs, two have been used as anchoring motifs for display of foreign proteins on host cell surfaces, namely, InaK from *P. syringae* KCTC1832 (Jung et al. 1998) and InaV from *P. syringae* INA5 (Schmid et al. 1997). Both intact INP and its truncated form of INC, with a deletion of the central repeating domain for reduction of the size, were shown to be able to display heterologous proteins on bacterial cell surface (Kim and Yoo 1998, 1999; Jung et al. 1998; Kwak et al. 1999; Kang et al. 2003). Even the N-terminal region alone could be employed as a potential cell surface display motif to direct translocation of foreign proteins to the cell surface (Li et al. 2004), and an important issue is that most cell surface display systems are limited in the size of passenger proteins, while the INP-based system could display proteins as large as 60 kDa (Sang et al. 2003), 77 kDa (Yim et al. 2006), and 90 kDa (Wu et al. 2006).

Y. Xu · Q. Liu · L. Zhou · Z. Yang · Y. Zhang (✉)
State Key Laboratory of Bioreactor Engineering,
East China University of Science and Technology,
130 Meilong Road, Shanghai 200237, China
e-mail: yxzhang@ecust.edu.cn

Vibrio anguillarum is a marine microbial pathogen infecting many commercial farmed fish and causes fatal hemorrhagic septicemic disease which results in massive death and great loss of profit in aquaculture around the world. In our previous work, several attenuated *V. anguillarum* strains derived from wild-type *V. anguillarum* strain MVM425 have been constructed. The strain MVAV6203, with the virulence-related plasmid pEIB1 (Wu et al. 2004) curing and an unmarked gene deletion of the *aroC*, was attenuated by 10,000 times and conferred excellent immune protection against *Vibrio* pathogens including *V. anguillarum* and *V. alginolyticus* in animal tests (unpublished). Therefore, MVAV6203 was considered to be an excellent live vaccine candidate. In this work, the attenuated *V. anguillarum* MVAV6203 was applied as the carrier host and succeeded in surface-anchoring the green fluorescent protein (GFP) with the aid of INP-based display systems, which is of great potential value for further multivalent carrier vaccine development.

Materials and Methods

Bacterial Strains and Plasmids

Escherichia coli TOP10 (Invitrogen, Carlsbad, CA, USA) was used for constructing recombinant plasmids. The genomic DNA of *P. syringae* pv. *syringae* (ICMP3023) provided full length of *inaV* gene. The attenuated *V. anguillarum* strain MVAV6203 developed in our previous work was used as the carrier host for surface display. Plasmid mTn*5gusA-pgfp21* carrying the *gfpuv* gene (Xi et al. 1999) provided the gene source for construction of GFP derivatives. Plasmid pUC18 (TaKaRa, Japan) was used as a parent plasmid for construction of truncated inaV hybrids. The strains and plasmids used in this study are shown in Table 1.

Plasmids Construction

Recombinant plasmids harboring various *inaV* hybrids were constructed as follows using the primers in Table 2. The genomic DNA of *P. syringae* pv. *syringae* (ICMP 3023) containing full length of *inaV* gene was used as a template to amplify the N- and C-terminal domain by using primer nos. 1–7. The amplified fragments were digested with corresponding enzymes and inserted into the same sites of plasmid vector pUC18 to generate three different display plasmids, named as pUC-Nhis, pUC-NChis, and pUC-NhisC. The 720 bp of *gfpuv* fragments was amplified from plasmid mTn*5gusA-pgfp*12 using primer nos. 8–12 and digested with corresponding enzymes and inserted into appropriate positions of the display plasmids to generate

Table 1 Strains and plasmids used in this study

Strains and plasmids	Relevant properties	Source
Strains		
Pseudomonas syringae ICMP3023	*P. syringae* pv. *syringae*	ICMP
Escherichia coli Top-10	Transformation host	Lab collection
Vibrio anguillarum MVAV6203	Attenuated strains, transformation host	This lab
VA(pG)	MVAV6203 derivative containing pUC-GFP	This study
VA(pNG)	MVAV6203 derivative containing pUC-NGFP	This study
VA(pNCG)	MVAV6203 derivative containing pUC-NCGFP	This study
VA(pNGC)	MVAV6203 derivative containing pUC-NGFPC	This study
Plasmids (ab.)		
pUC18	*E. coli* cloning vector, *lac* promoter, Ap^r	TaKaRa
mTn*5gusA-pgfp21*	gfp containing mini-Tn5 transposon derivative	Xi et al. (1999)
pUC-GFP (pG)	pUC18 derivative containing 0.7 kb GFP gene, Ap^r	This study
pUC-Nh (pNh)	pUC18 derivative containing 0.6 kb *inaV*N gene, Ap^r	This study
pUC-NCh (pNCh)	pUC18 derivative containing 0.9 kb *inaV*NC gene, Ap^r	This study
pUC-NhC (pNhC)	pUC18 derivative containing 0.9 kb *inaV*NC gene, Ap^r	This study
pUC-NGFP (pNG)	pUC-Nh derivative containing 0.7 kb GFP gene, Ap^r	This study
pUC-NCGFP (pNCG)	pUC-NCh derivative containing 0.7 kb GFP gene, Ap^r	This study
pUC-NGFPC (pNGC)	pUC-NhC derivative containing 0.7 kb GFP gene, Ap^r	This study

Table 2 Primers used in the construction

Primer no.	Primer name	Sequence (5′–3′)
1	PinaN5'E	GCC*GAATTC*TGAGGATGCTGTAATGAA
2	PinaNh3'K	TCTAGAC*GGTACC*ATGATGATGATGATGATGAATCAGATCACTGTGGTTGCCAG
3	PinaN3'K	GCC*GGTACC*AATCAGATCACTGTG
4	PinaC5'K	GTA*GGTACC*GGCGGGCATGACTGC
5	PinaCh3'B	TCTAGAC*GGATCC*ATGATGATGATGATGATGGAGCTCGACCTCTATCCAGT
6	PinaC5'B	GTA*GGATCC*GGCGGGCATGACTGC
7	PinaC3'P	CGA*CTGCAG*CTAGAGCTCGACCTCTATCCAGT
8	PGFP5'K	GGC*GGTACC*ATGGCTAGCAAAGGAGAA
9	PGFP3'P	GGG*CTGCAG*TTATTTGTACAGTTCATC
10	PGFP5'B	GGC*GGATCC*ATGGCTAGCAAAGGAGAA
11	PGFP3'B	GGG*GGATCC*TTTGTACAGTTCATC
12	PGFP5'E	GCC*GAATTC*GAATGGCTAGCAAAGGAGAA

three reporter plasmids named: pUC-NGFP, pUC-NCGFP, and pUC-NGFPC (Fig. 1). The cytosolic GFP expression plasmid was also constructed by fusion the *gfp* gene into the MCS of pUC18 by *Eco*RI and *Pst*I digestion, which resulted in the pUC-GFP as a control plasmid for either expression or localization assays.

Culture Condition and Fusion Protein Expression

The *E. coli* TOP10 strain harboring plasmid was grown in Luria–Bertani (LB) medium (Tryptone 1%, yeast extract

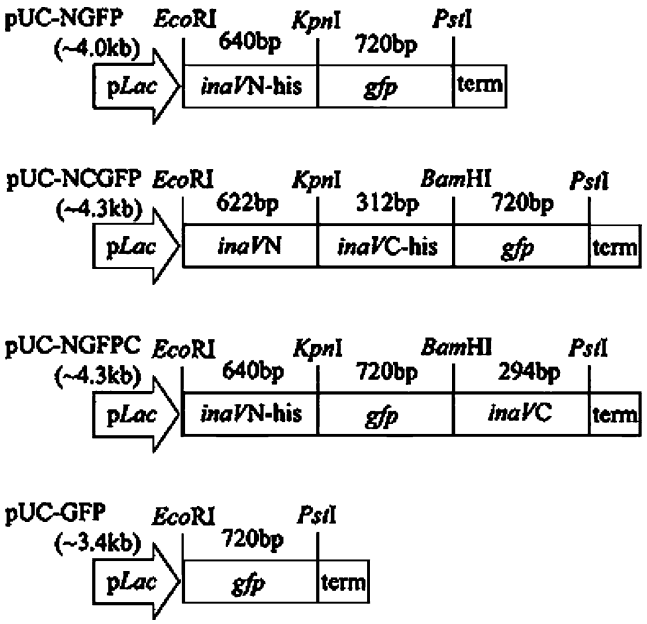

Fig. 1 Gene maps of recombinant plasmids harboring truncated *inaV*-GFPuv fusion constructs. Plasmid pUC18 was used as a parent vector for constructing these fusions. p*Lac*, *lac* promoter; *inaV*, ice nucleation protein gene; *inaV*N, N-terminal domain of *inaV*; *inaV*N-his, N-terminal domain of *inaV* with his-tag; *inaV*C, C-terminal domain of *inaV*; *inaV*C-his, C-terminal domain of *inaV* with his-tag; *gfp*, UV-optimized green fluorescent protein gene; term, termination sequence

0.5%, NaCl 0.5%) supplemented with ampicillin to a final concentration of 100 μg/ml. Cells were grown in 250-ml flasks with a 50-ml working volume in a shaker at 200 rpm and 37°C. The *V. anguillarum* strain MVAV6203 harboring plasmid was grown in LB2 medium (Tryptone 1%, yeast extract 0.5%, NaCl 2%) supplemented with ampicillin to a final concentration of 200 μg/ml. Cells were grown in 250-ml flasks with a 50-ml working volume in a shaker at 200 rpm and 30°C. For expression, overnight cultures were subcultured at 1:100 and cultured at 30°C for 1 day.

Measurement of Whole Cell Fluorescence

Cell density (OD600) was measured at 600 nm on an ultraviolet–visible (UV/Vis) spectrophotometer. The whole cell GFP fluorescence was determined by a fluorescence microplate reader (GENios Pro, Tecan, Mannedorf, Zurich, Switzerland) at excitation of 485 nm and emission at 535 nm. All the samples were diluted to OD600 of 1.0 before fluorescence was measured using the phosphate-buffered saline (PBS). The fluorescence signal of the untransformed cells of attenuated *V. anguillarum* strain diluted under the same condition (OD600=1.0) was set as background and subtracted from the overall fluorescence to give the GFP fluorescence. For comparison, all the GFP fluorescence data were normalized by the average fluorescence signal.

Cell Fractionation

Bacterial cell fractionation was performed by the sodium lauroyl sarcosine (SLS) method with minor modifications (Lattemann et al. 2000). Cells harboring display plasmid were cultured for 24 h. Cells were harvested by centrifugation at 10,000×*g* for 2 min, washed by PBS three times, and resuspended in Tris-HCl buffer (50 mM, pH 8.0, containing 0.3% NaCl). The cell suspension was, then,

treated with an ultrasound sonication for 5 min on ice. To remove unbroken cells and debris, the whole cell lysate was centrifuged at 5,000×*g* for 5 min. To obtain total membrane fraction, the supernatant was pelleted by centrifugation at 20,000×*g* and 4°C for 1 h using an ultracentrifuge (Sigma, Osterode, Germany). The supernatant was regarded as soluble cytoplasmic fraction. For further outer membrane fractionation, the pellet (total membrane fraction) was resuspended with 4-(2-hydroxyethyl)-1-piperazineethanesulfonic acid buffer (10 mM, pH 7.4) containing 1% SLS for solubilizing inner membrane and incubated at room temperature for 30 min, and then the outer membrane fraction was repelleted by ultracentrifugation for 1 h at 20,000×*g* and 4°C. The supernatant was regarded as the inner membrane fraction, and after a repeat for outer membrane fractionation, the pellet was regarded as the outer membrane fraction. After cell fractionation, equal volumes of the cytoplasmic fraction and outer membrane fraction were saved for further analyses.

Enzyme-Linked ImmunoSorbent Assay

The cytoplasmic fraction and outer membrane fraction were all diluted to the same OD (OD 280 nm=1.0) on a NanoDrop ND-1000 UV-Vis spectrophotometer (NanoDrop Technologies, USA). Microtitre plate wells were coated with 50 μl of each fraction solution by overnight incubation at 4°C. Excess protein was discarded and wells were blocked with 200 μl of PBS containing 3% bovine serum albumin (BSA) for 1 h at 37°C. After removing the blocking solution and washing three times with PBS-T (PBS buffer, pH 7.2, containing 0.05% Tween-20), the wells were incubated for 1.5 h at 37°C with rabbit-anti-GFP (Proteintech, USA) antibody at a dilution of 1:5,000 (*v*/*v*). The complex were washed three times with PBS-T and then incubated for 1.5 h at 37°C with horseradish peroxidase-conjugated goat-anti-rabbit antibody (Jackson ImmunoResearch Laboratories, USA) at a dilution of 1:10,000 (*v*/*v*). Finally, the wells were washed three times again, and (3,3′,5,5′-Tetramethylbenzidine) TMB solution (TIANGEN Biotech, Beijing, China) was added as a color-developing substrate. With the addition of 2 M H_2SO_4, the reaction was terminated. The absorbance of each well was measured at 450 nm by a microplate reader (Bio-Rad model 550, Hercules, CA, USA).

Sodium Dodecyl Sulfate-Polyacrylamide Gel Electrophoresis and Western Blot

The cell fraction (cytoplasmic and outer membrane) in equal volume was mixed with sample loading buffer, boiled for 5 min, and resolved by 12% sodium dodecyl sulfate-polyacrylamide gel electrophoresis. For western blot analysis, gel was electroblotted onto polyvinylidene-fluoride membrane using a Mini Protean 3 Cell (Bio-Rad, Hercules, CA, USA) at 100 V for 3 h. The membrane was then blocked with PBS-T-BSA buffer (PBS buffer, pH 7.2, containing 0.05% Tween-20 and 2% (*w*/*v*) BSA) at 37°C for 1 h. For immunodetection, the membrane was incubated for 1.5 h at 37°C in antibody solution (PBS-T-BSA buffer) containing polyclonal rabbit-anti-GFP antibody (1:3,000 (*v*/*v*); Proteintech) and probed with secondary goat-anti-rabbit immunoglobulin G conjugated with horseradish peroxidase (1:5,000 (*v*/*v*); Jackson ImmunoResearch Laboratories). After successive washing with PBS-T, the TMB solution (TIANGEN Biotech) was added and the reaction was quenched with 2 M H_2SO_4.

Results

Expression of GFP Fusion Proteins

To display GFP on the surface of attenuated *V. anguillarum* strain MVAV6203, we constructed different recombinant surface display plasmids of pUC-NGFP, pUC-NCGFP, and pUC-NGFPC that direct the expression of corresponding fusion proteins. The plasmids encoded different combinations of a truncated INP and GFP (Fig. 1). The GFP cytosolic expression plasmid pUC-GFP was constructed as a control. All the recombinant plasmids were transformed into attenuated *V. anguillarum* strain MVAV6203 by electroporation, generating the reporter strains of VA(pNG), VA(pNCG), and VA(pNGC) for GFP outer-membrane anchoring as well as VA(pG) for GFP cytosolic expression. All the transformed reporter strains were found to be

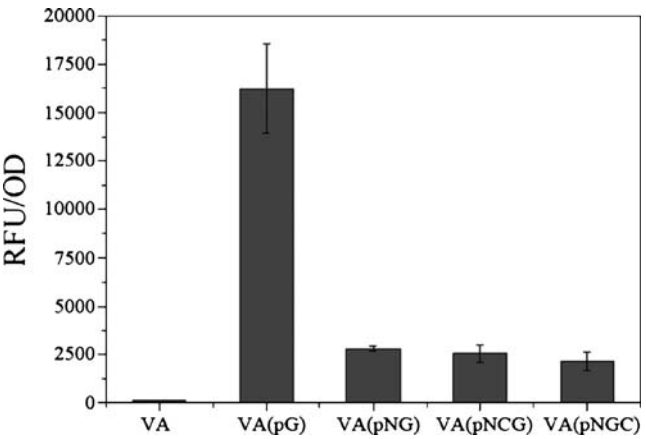

Fig. 2 Total GFP expression of different reporter strains. VA, attenuated *V. anguillarum* strains MVAV6203; VA(pG), reporter strain for GFP cytosolic expression; VA(pNG), VA(pNCG), VA(pNGC), reporter strains for GFP outer membrane display. Cells were grown at LB2 medium at 30°C for 24 h. The GFP fluorescence was determined by GENios Pro at excitation of 485 nm and emission at 535 nm

fluorescent upon UV illumination, or by fluorescence microscopic observation, indicating that GFP variants were functionally expressed when fused with the truncated INP.

The specific expression level of each GFP sample was determined by whole cell fluorescence intensity based on unit cell density (OD600=1). The GFP expression showed no difference among the strains with or without inducement of 0.1 mM IPTG in *V. anguillarum* (Data not shown). The total GFP expression of different strains was shown in Fig. 2. Compared with VA(pG), the display strains of VA(pNG), VA(pNCG) and VA(pNGC) had obvious loss in fluorescence, indicating the production of truncated INP-GFP fusion proteins was much lower than that of the cytosolic expressed GFP.

Surface Localization of Fusion Proteins

In order to examine the expression and the localization of fusion proteins, harvested cells were divided into an outer membrane fraction and a soluble cytoplasmic fraction and then subjected to Enzyme-Linked ImmunoSorbent Assay (ELISA) and western blot assays. Because all the samples were diluted to the same level (OD 280 nm=1) in ELISA analysis, the OD values represented the relative amount of GFP fusions of total proteins in either the cytoplasmic fraction or the membrane fraction. Compared with the negative control VA, the cytosolic expression strain VA(pG) only produced GFP in the cytoplasmic fraction, while the outer membrane display strains VA(pNG), VA(pNCG), and VA(pNGC) expressed the GFP fusions both in the cytoplasmic and outer membrane fractions (Fig. 3). Also, their efficiency of translocation were at similar levels, indicating the anchoring motifs from INP succeeded in translocating part of the GFP fusions onto the cell surface of the marine bacterial host *V. anguillarum*.

For detailed analysis of surface localization, equal volumes of subcellular fractions of different samples were subjected to western blot analysis. The GFP band (27 kDa) expressed by VA(pG) was found only in the cytoplasmic fraction and not in the outer membrane fraction (below detection levels, Fig. 4, lanes 1 and 2). The fusion proteins of NGFP (49 kDa), NCGFP (60 kDa), and NGFPC (60 kDa) could be found in both cytoplasmic fractions and outer membrane fractions (Fig. 4, lanes 3 to 8), indicating only part of the fusion proteins were translocated onto the outer membrane of the bacterium. The GFP fusion proteins detected in the cytoplasmic fractions presented different degradation products with the estimated size of 27, 31, and 33 kDa (Fig. 4, lanes 3, 5, 7), while no GFP-containing degradation product was detected in the outer membrane fractions (Fig. 4, lanes 4, 6, 8). Interestingly, it was also observed that the GFP fusion proteins in outer membrane fractions were a bit larger in size than their corresponding bands in cytoplasmic fractions and the reason for this is currently unknown (Fig. 4).

Time Course of Display System N-GFP

For developing multivalent live vaccine in attenuated *V. anguillarum* strain by INP-based antigen display system, the excellent candidate display system N-GFP was selected and its time course in protein expression and display was further analyzed.

The cell growth and specific GFP expression of VA(pNG) were first examined. During the growth of VA(pG) and VA(pNG), there was a slight longer lag phase than that of the control VA (data not shown). And, as mentioned above (Fig. 2), the production of N-GFP fusion protein was much lower than that of the cytosolic-expressed GFP during the whole growth phase. Further assay for GFP display in

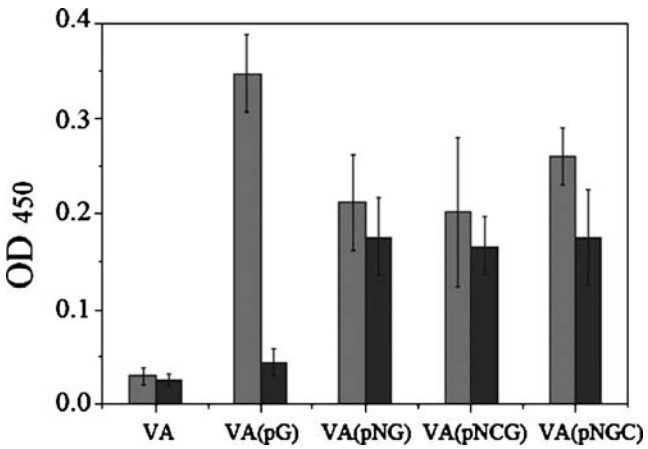

Fig. 3 ELISA analysis for cytoplasmic fraction (*light gray bars*) and outer membrane fraction (*dark gray bars*) of reporter strains. The samples were all diluted to the same level (OD 280 nm=1). Cells were cultured in LB2 medium at 30°C for 24 h and followed by fractionation

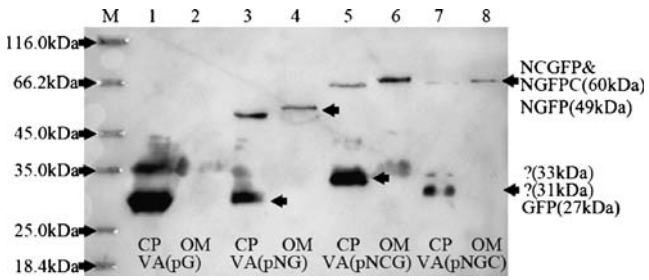

Fig. 4 Western blot results of different fractions of reporter strains (*CP*: cytoplasmic fraction; *OM*: outer membrane fraction). *M*, prestained protein molecular weight marker (MBI Fermentas); *lanes 1* and *2*, CP and OM fractions of VA(pG); *lanes 3* and *4*, CP and OM fractions of VA(pNG); *lanes 5* and *6*, CP and OM fractions of VA(pNCG); *lanes 7* and *8*, CP and OM fractions of VA(pNGC)

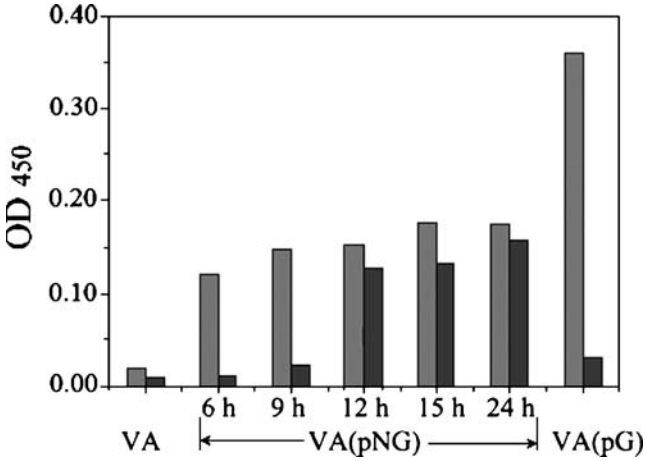

Fig. 5 ELISA analysis for cytoplasmic fraction (*light gray bars*) and outer membrane fraction (*dark gray bars*) of reporter strain VA(pNG). The samples were diluted to the same level (OD 280 nm=1). Cells were cultured in LB2 medium at 30°C for 24 h and followed by fractionation

VA(pNG) was carried out. Different subcellular fractions of VA(pNG) at 6, 9, 12, 15, and 24 h were diluted to the same level (OD 280 nm=1) and, then, subjected to ELISA analysis. Compared with VA and VA(pG), the VA(pNG) presented a GFP signal in the cytoplasmic fraction after 6 h of culture, and the expression of cytosolic GFP increased until 15 h of culture (Fig. 5, light gray bars). While in the outer membrane fraction, the GFP signal appeared at 12 h and slightly increased during 12–24 h (Fig. 5, dark gray bars).

At the same time, equal volumes of subcellular fractions of VA(pNG) at 6, 9, 12, 15, and 24 h were also analyzed by western blot. The VA(pG) presented a very thick GFP band of 27 kDa in the cytoplasmic fraction and no obvious band in the outer membrane fraction. In all the cytoplasmic fractions of VA(pNG), there were a 49 kDa N-GFP band and also a 27 kDa GFP band probably caused by degradation. Agreeing with the results in Fig. 5, the N-GFP did not appear in the outer membrane fraction until 12 h of culture, indicating that the translocation obviously lagged behind the protein expression. By density scanning of the western blot patterns, the amounts of translocated N-GFP and cytoplasmic GFP increased along with time and reached the maximum at 24 h. Also, the degradation products in cytoplasmic fraction increased rapidly after 15 h (Fig. 6, lane 11). The N-GFP fusions in outer membrane fractions were consistently a little larger in size than those in cytoplasmic fractions under unknown mechanism.

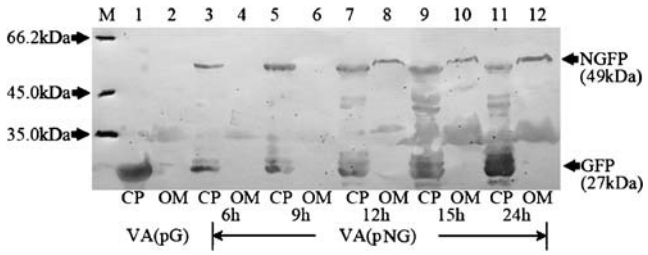

Fig. 6 Western blot analysis of different fractions of VA(pNG) along with time. *M*, prestained protein molecular weight marker (MBI Fermentas); *lanes 1* and *2*, CP and OM fractions of VA(pG) at 24 h; *lanes 3* and *4*, CP and OM fractions of VA(pNG) at 6 h; *lanes 5* and *6*, CP and OM fractions of VA(pNG) at 9 h; *lanes 7* and *8*, CP and OM fractions of VA(pNG) at 12 h; *lanes 9* and *10*, CP and OM fractions of VA(pNG) at 15 h; *lanes 11* and *12*, CP and OM fractions of VA(pNG) at 24 h

Discussion

In this study, we constructed different forms of display systems upon *P. syringae* truncated ice nucleation protein to direct and display green fluorescence protein onto the cell surface of attenuated *V. anguillarum* strain MVAV6203. The 609 bp N-terminal domain and 300 bp C-terminal domain of INP from *P. syringae* ICMP 3023 were amplified and aligned with other sequences of different strains of *P. syringae*. Compared with the protein sequence of InaV (derived from *P. syringae* INA5; Schmid et al. 1997), InaK (derived from *P. syringae* KCTC1832; Li et al. 2004), and InaZ (derived from *P. syringae* pv. *syringae* B728a; Miller et al. 2000), the truncated INP in this work was proximal with InaV at about 94% homology, so we recognized this protein derived from *P. syringae* ICMP 3023 as InaV.

Compared with the *E. coli* Top-10 strain in which *lac* promoter was strictly induced by IPTG, there was no difference between the expression levels of heterologous proteins in *V. anguillarum* reporter strains with and without IPTG induction. This demonstrated that the *lac* promoter became a constitutive promoter in *V. anguillarum*, probably due to the absence in the genome of a *lacI* gene encoding a repressor protein (Shao et al. 2005). IPTG-independent expression and display of heterologous proteins in *V. anguillarum* will be of benefit to simplify the cell culture processes and very important in the application of carrier vaccine.

For assaying surface localization of fusion protein expressed by each reporter strain, collected cells were fractionated and subsequently analyzed by ELISA and western blot. The GFP produced by the cytoplasmic expression strain VA(pG) was found only in the cytoplasmic fraction and not in the outer membrane fraction. This proved that the subcellular fractionation was successfully performed, and no cytoplasmic component was mixed into the outer membrane fraction. When fused with truncated INP, the GFP could be detected in both cytoplasmic fraction and outer membrane fraction, and part of the expressed GFP

fusions could be successfully translocated onto the outer membrane of *V. anguillarum* by INP-based anchoring motifs.

The GFP fusion proteins showed signs of extensive proteolysis as there were different degradation products in the cytoplasmic fractions but not in the outer membrane fractions. This suggested that the fusion proteins showed completely good structural stability when functionally displayed onto the cell surface of *V. anguillarum*.

The previously reported that *InaK* derivative NC-GFP fusion protein had a 32-kDa degradation product in the cytoplasmic fraction and was presumed as GFP conjugated with C domain (Li et al. 2004). In this work, the degradation products in the cytoplasmic fractions were mainly 27 kDa GFP and two GFP-containing proteins of 31 kDa and 33 kDa with smaller size than the predicted C-GFP fusion of 37 kDa (Fig. 4, lanes 3, 5, 7). We assumed that there might be proteolysis sites in the fusion proteins, generating degradation products of different sizes (Fig. 4, lanes 3, 5, 7). As degradation products existed in all the display systems, it was believed that better cell surface display efficiency could be achieved if fusion proteins could be protected from proteolysis in the cytoplasm (Li et al. 2004).

According to the estimated ratio of displayed protein to expressed protein, the translocation efficiency is rather low. However, the low translocation efficiency may be due to the space hindrance on the outer membrane. As shown in Fig. 5, when the cytoplasmic and outer membrane fractions were equally diluted to the same level (OD 280 nm=1), the GFP fusions in both fractions were presented at the same level. In other words, displayed fusions accounted for a similar percentage in total outer membrane fractions as cytoplasmic fusions did in total cytoplasmic fractions. Therefore, we consider that the absolute translocation efficiency for a surface display system could not reach a high level because it is easy to understand that a limited cell surface cannot hold so many heterologous proteins before reaching its saturated situation.

Like other anchoring motifs that displayed the GFP onto the cell surface of *E. coli* (Shi and Su 2001), the display of GFP on the *V. anguillarum* cell surface also resulted in destabilization of the membrane integrity. This membrane destabilization was reported to be a general consequence in heterologous proteins display. Therefore, we believe it was better for the bacterial cells to express and display heterologous protein moderately so that the strain would have high viability with stable membrane for further applications in live carrier vaccine development.

In conclusion, we constructed and compared the abilities of three forms of display systems derived from *P. syringae*-truncated INP to direct and display GFP onto the cell surface in attenuated *V. anguillarum* strain MVAV6203. The three display systems showed similar cell surface display ability and efficiency, and the total expression and surface display levels of N-GFP system were higher and more stable than the other two when based on unit cell density. Time course of the N-GFP system demonstrated that there was a lag of 6 h between expression and translocation of the N-GFP fusion in *V. anguillarum* strain MVAV6203. The degradation products of GFP fusions were found in cytoplasmic fractions and increased with time. By now, preliminary developments of carrier vaccines in G bacterial host based on surface display have been reported mainly in *E. coli* and *Salmonella typhi* against human disease (Kim and Yoo 1999; Lee et al. 2000; Kang et al 2003), but similar vaccine developments in marine bacteria have not been reported yet. In this work, we explored the feasibility of the INP-directed display systems in *V. anguillarum*. Our results proved that the truncated INP display systems could be used in the attenuated *V. anguillarum* strain and may serve for further multivalent carrier vaccine development by display protective antigens from different pathogens.

Acknowledgments The work was supported by National Natural Science Foundation of China (30600460) and National High Technology Research and Development Program of China (2006AA100310).

References

Boder ET, Wittrup KD (1997) Yeast surface display for screening combinatorial polypeptide libraries. Nat Biotechnol 15:553–557

Catherine MHC, Mulchandani A, Chen W (2002) Bacterial cell surface display of organophosphorus hydrolase for selective screening of improved hydrolysis of organophosphate nerve agents. Appl Environ Microbiol 68:2026–2030

Graether SP, Jia ZC (2001) Modeling pseudomonas syringae ice-nucleation protein as a beta-helical protein. Biophys J 80: 1169–1173

Jung HC, Park JH, Park SH, Lebeault JM, Pan JG (1998) Expression of carboxymethylcellulase on the surface of *Escherichia coli* using *Pseudomonas syringae* ice nucleation protein. Enzyme Microbiol Technol 22:348–354

Kang SM, Rhee JK, Kim EJ, Han KH, Oh JW (2003) Bacterial cell surface display for epitope mapping of hepatitis C virus core antigen. FEMS Microbiol Lett 226:347–353

Kim EJ, Yoo SK (1998) Cell surface display of CD8 ecto domain on *Escherichia coli* using ice nucleation protein. Biotechnol Tech 12:197–201

Kim EJ, Yoo SK (1999) Cell surface display of hepatitis B virus surface antigen by using *Pseudomonas syringae* ice nucleation protein. Lett Appl Microbiol 29:292–297

Kwak YD, Yoo SK, Kim EJ (1999) Cell surface display of human immunodeficiency virus type 1 gp120 on *Escherichia coli* by using ice nucleation protein. Clin Diagn Lab Immun 6:499–503

Lattemann CT, Maurer J, Gerland E (2000) Autodisplay: functional display of active β-lactamase on the surface of *Escherichia coli* by the AIDA-I autotransporter. J Bacteriol 182:3726–3733

Lee JS, Shin KS, Pan JG, Kim CJ (2000) Surface-displayed viral antigens on Salmonella carrier vaccine. Nat Biotechnol 18:645–648

Li L, Kang DG, Cha HJ (2004) Functional display of foreign protein on surface of *Escherichia coli* using N-terminal domain of ice nucleation protein. Biotechnol Bioeng 85:214–221

Liljeqvist S, Samuelson P, Hansson M, Nguyen TN, Binz H, Stahl S (1997) Surface display of the cholera toxin B subunit on *Staphylococcus xylosus* and *Staphylococcus carnosus*. Appl Environ Microbiol 63:2481–2488

Miller WG, Leveau JH, Lindow SE (2000) Improved gfp and inaZ broad-host-range promoter-probe vectors. Mol Plant Microbe Interact 13:1243–1250

Richins RD, Kaneva I, Mulchandani A, Che W (1997) Biodegradation of organophosphorus pesticides by surface-expressed organophosphorus hydrolase. Nat Biotechnol 15:984–987

Sang YL, Jong HC, Xu ZH (2003) Microbial cell-surface display. TRENDS Biotechnol 21:45–52

Schmid D, Pridmore D, Capitani G, Battistutta R, Neeser JR, Jann A (1997) Molecular organization of the ice nucleation protein InaV from *Pseudomonas syringae*. FEBS Lett 414:590–594

Shao MF, Ma Y, Liu Q, Zhang YX (2005) Secretory expression of recombinant proteins in an attenuated *Vibrio anguillarum* strain for potential use in vaccines. J Fish Dis 28:723–728

Shi HD, Su WW (2001) Display of green fluorescent protein on *Escherichia coli* cell surface. Enzyme Microb Tech 28:25–34

Wu HZ, Ma Y, Zhang YX, Zhang HZ (2004) Complete sequence of virulence plasmid pEIB1 from the marine fish pathogen *Vibrio anguillarum* strain MVM425 and location of its replication region. J Appl Microbiol 97:1021–1028

Wu ML, Tsai CY, Chen TH (2006) Cell surface display of Chi92 on *Escherichia coli* using ice nucleation protein for improved catalytic and antifungal activity. FEMS Microbiol Lett 256: 119–125

Xi CW, Lambrecht M, Vanderleyden J, Michiels J (1999) Bifunctional gfp-and gusA-containing mini-Tn5 transposon derivatives for combined gene expression and bacterial localization studies. J Microbiol Meth 35:85–92

Xu Z, Lee SY (1999) Display of polyhistidine peptides on the *Escherichia coli* cell surface by using outer membrane protein C as an anchoring motif. Appl Environ Microbiol 65: 5142–5147

Yim SK, Jung HC, Pan JG, Kang HS, Ahn T, Yun CH (2006) Functional expression of mammalian NADPH-cytochrome P450 oxidoreductase on the cell surface of *Escherichia coli*. Protein Expr Purif 49:292–298